Letters

Compact Rectifiers With Ultra-wide Input Power Range Based on Nonlinear Impedance Characteristics of Schottky Diodes

Zhongqi He, *Student Member, IEEE*, Jing Lan, and Changjun Liu, *Senior Member, IEEE*

***Abstract*—Two high-efficiency radio-frequency (RF) rectifiers with extended input power range are proposed by taking the advantage of nonlinear impedance characteristics of diodes. Each rectifier consists of two subrectifiers that operates at high- and low-power levels, respectively. A nonlinear power division strategy is applied to the input power level without any power dividers or couplers. A λ/8 transmission line is introduced to compensate the imaginary part of diode impedance. A λ/4 transmission line is applied to reverse the diode impedance variation with respect to the input power. Two rectifiers operating at 2.45 GHz are fabricated and measured. Rectifier I shows a RF-dc power conversion efficiency exceeding 50% over an input power range of 23.3 dB (from 6.5 to 29.8 dBm), with maximum efficiency 74.5% at 27 dBm input power. Rectifier II shows an input power range exceeding 50% over 31 dB (−1 to 30 dBm) with maximum efficiency of 68.5% at 28 dBm.**

***Index Terms*—High efficiency, input power range, nonlinear, Schottky Diodes, wireless power transmission (WPT).**

I. Introduction

RECTIFIERS are important components in wireless power transmission (WPT) systems based on electromagnetic coupling [1], [2] or antenna radiation [3], [4]. High RF-dc conversion efficiency is the essential requirement for a rectifier and is closely related to the performance of a WPT system [5]. Recently, WPT over a wide power range has become increasingly popular because the input power is not constant in most WPT systems [6], such as the application for charging unmanned aerial vehicle [7]. In order to achieve wide power range, the efficiency and complexity of the rectifier are usually sacrificed.

Some research teams used different design methods to improve the performance of their rectifiers over wide input power ranges. In [8], Shinohara *et al.* presented a sequential power delivery technique to enhance the dynamic power range of a rectifier successfully. In [9], an integrated impedance compression network was proposed to enhance the power range. In [10], a balanced novel RF rectifier was introduced to recycle the power dissipated in the resistances. In [11], a self-tuning impedance matching structure was proposed to obtain an extended input power range for a rectifier.

These existing solutions may cause more insertion loss, need extra circuit board space, and lead to circuit complex. In this letter, we present two high-efficiency rectifiers with wide power ranges by taking advantage of nonlinear impedance characteristics of diodes. These rectifiers consist of three diodes, which are used in two parallel subrectifiers. The input power is divided into high- and low-input power levels based on the input power level. A facilitated rectifier topology is realized and results in reduction of the insertion loss and circuit size.

Manuscript received October 29, 2020; revised November 29, 2020; accepted December 16, 2020. Date of publication December 21, 2020; date of current version March 5, 2021. This work was supported in part by the National Natural Science Foundation of China under Grant 62071316. *(Corresponding author: Changjun Liu.)*

The authors are with the School of Electronics and Information Engineering, Sichuan University, Chengdu 610064, China (e-mail: 1141511223@qq.com; 555978@qq.com; cjliu@ieee.org).

Color versions of one or more of the figures in this article are available online at https://doi.org/10.1109/TPEL.2020.3046083.

Digital Object Identifier 10.1109/TPEL.2020.3046083

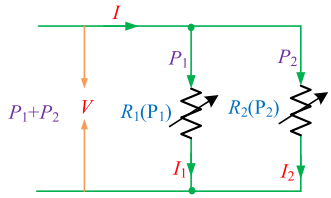

Fig. 1. Simplified mode of two shunt nonlinear resistances.

II. Design Principle Based on Nonlinear Impedance Characteristic

A. Basic Principle of Power Dividing

Assume that there is a nonlinear resistance R, which is dependent on the applied power P as

$$R(P) = k_0 \ln\left(\frac{P}{P_0}\right) \tag{1}$$

where k_0 and P_0 are two constants. We have two nonlinear resistance as shown in Fig. 1. Since two resistance share the same voltage, the power ratio between them is

$$\frac{P_1}{P_2} = \frac{R_2(P_2)}{R_1(P_1)}. \tag{2}$$

When $R_2 = R_1$, it leads to a balanced power division.

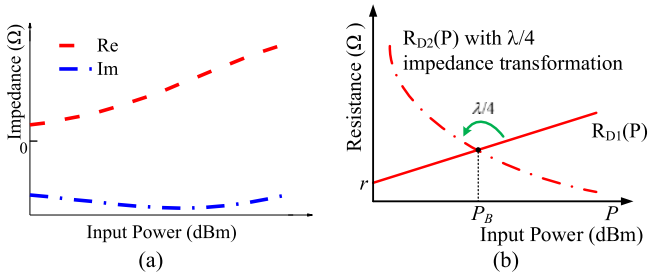

Fig. 2. (a) Impedance of diode HSMS282 varies with input power at 2.45 GHz with RL = 400 Ω. (b) Resistances vary with input power.

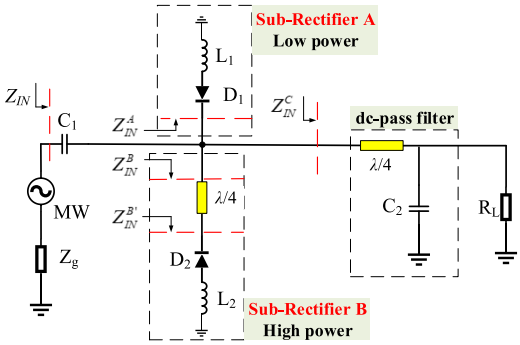

Fig. 3. Block diagram of power division strategy that includes two subrectifiers.

B. Nonlinear Impedance of Diodes

From K. Chang's nonlinear diode model, the input impedance of a Schottky diode at a fixed load is [12]

$$Z_D = \frac{\pi R_s}{\cos\theta_{on}\left(\frac{\theta_{on}}{\cos\theta_{on}} - \sin\theta_{on}\right) + j\omega R_s C_j\left(\frac{\pi-\theta_{on}}{\cos\theta_{on}} + \sin\theta_{on}\right)} \tag{3}$$

where R_s is the series resistance of the diode, θ_{on} is the turn-ON angle of the diode, and C_j is the junction capacitance of the diode. From (3), the impedance of a HSMS282 diode is shown in Fig. 2(a). Then, we may use a series inductance to balance the diode capacitance, then the diode impedance will tune to be almost pure resistance.

C. Rectifying Circuit Realization

Ideally, we suppose there are two parallel subrectifiers (A and B) with the same structures of a diode and an inductance in series, which is to compensate the imaginary part of the diode. A block diagram of the proposed rectifier is shown in Fig. 3.

We can use a simple power division principle to design high efficiency rectifier with wide input power range by changing resistances of different subrectifiers.

The principle of the power division strategy is as follows.

1) When the input power is low $P_{in} \ll P_B$, we have $\mathrm{Re}(Z_{D1}) = \mathrm{Re}(Z_{D2}) \ll Z_0$, where Z_{D1} and Z_{D2} are the impedances of diodes D_1 and D_2, respectively, as shown in Fig. 2(a). L_1 and L_2 are used to compensate the imaginary parts of the diodes' impedance causing Z_{IN}^A and $Z_{IN}^{B'}$ showing pure resistances. With the λ/4 transmission line (as an impedance transformer) in subrectifier B, $\mathrm{Re}(Z_{IN}^{B'})$ is transformed to a high value as shown in Fig. 2(b). According to the transmission line theory, we have $\mathrm{Re}(Z_{IN}^A) = R_{D1}$ and $\mathrm{Re}(Z_{IN}^B) = Z_1^2 / R_{D2}$, where Z_1 is the characteristic impedance of the λ/4 transmission line in subrectifier B. By selecting the value of Z_1 carefully, we have $\mathrm{Re}(Z_{IN}^A) << \mathrm{Re}(Z_{IN}^B)$, which leads the power ratio as follows:

$$\frac{P_B}{P_A} = \frac{\mathrm{Re}(Z_{IN}^A)}{\mathrm{Re}(Z_{IN}^B)} = \frac{R_{D1}\cdot R_{D2}}{Z_1^2} \ll 1. \tag{4}$$

2) When the input power is around P_B, we have $\mathrm{Re}(Z_{IN}^A) = \mathrm{Re}(Z_{IN}^B)$, which leads the power ratio as follows:

$$\frac{P_B}{P_A} = \frac{\mathrm{Re}(Z_{IN}^A)}{\mathrm{Re}(Z_{IN}^B)} = \frac{R_{D1}\cdot R_{D2}}{Z_1^2} \approx 1. \tag{5}$$

3) When the input power is high $P_B \ll P_{in}$, the real part of a diode's impedance usually is high. We have $\mathrm{Re}[Z_{D1}] = \mathrm{Re}[Z_{D2}] >> Z_0$. With the impedance transformer in subrectifier B, the real part of the input impedance of subrectifier B is transformed to a low impedance. Thus, we have $\mathrm{Re}(Z_{IN}^A) >> \mathrm{Re}(Z_{IN}^B)$, which leads the power ratio as follows:

$$\frac{P_B}{P_A} = \frac{\mathrm{Re}(Z_{IN}^A)}{\mathrm{Re}(Z_{IN}^B)} = \frac{R_{D1}\cdot R_{D2}}{Z_1^2} \gg 1. \tag{6}$$

We can tune the characteristic impedance and the length of the microstrip lines in subrectifier B and the value of L_1 and L_2 to adjust the power ratio in all three states.

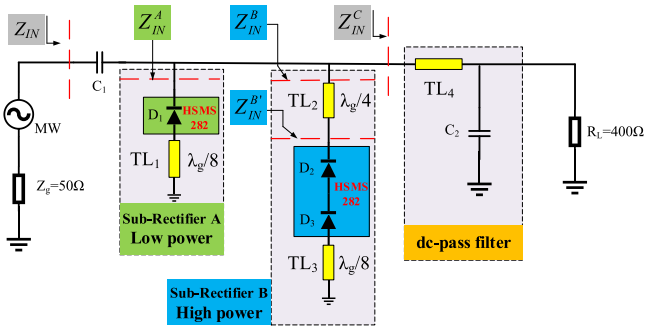

Fig. 4. Schematic of proposed rectifier I with power division diode array.

III. Design, Simulation, and Measurement of Rectifier I

In order to increase the dynamic power range of a microwave rectifier, we should choose two different diodes, e.g., D_1 for low power and D_2 for high power situation as shown in Fig. 3. A method to build a large power diode is to series two diodes. Thus, we use one HSMS282 for D_1 and two HSMS282 for D_2.

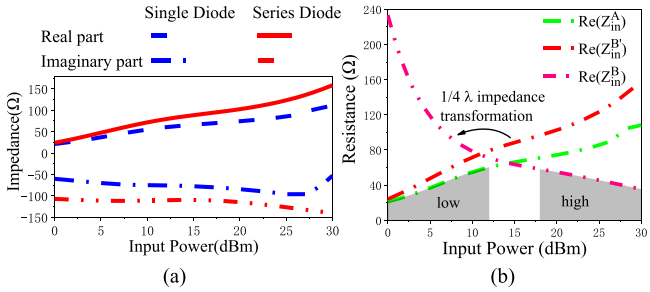

Fig. 5. (a) Input impedance of one single and two series HSMS-282 diodes based on SPICE models. (b) Re(Z_{IN}^{A}) and Re(Z_{IN}^{B}) and Re($Z_{IN}^{B'}$) versus input power.

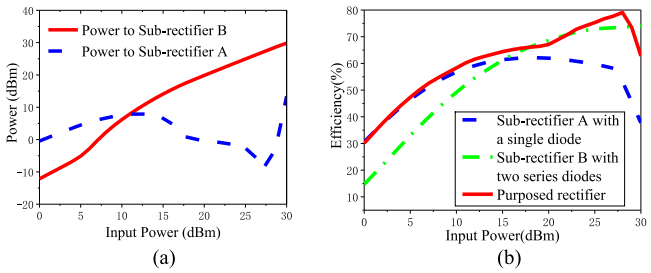

Fig. 6. (a) Power division strategy of rectifier I. (b) Simulated efficiency of rectifier I when comparing with one and two diodes operating individually.

A. Design Methodology

The proposed rectifier I is shown in Fig. 4. Two short-circuit stubs, TL_1 and TL_3, are introduced in subrectifier A and subrectifier B, respectively, to be used as inductors to compensate the imaginary parts of the diodes' impedance. One transmission line segment (TL_2) is proposed to transform Re(Z_{IN}^{B}) into Z_g at high input power.

The proposed rectifier I uses the nonlinear input impedance of a diode to realize the power division strategy. The diodes in subrectifier A and subrectifier B show power-related input impedances. Because the number of diodes used is different, their input impedances vary differently with the input power. Fig. 5(a) shows the input impedances of one single and two series HSMS-282 diodes for different input powers. The imaginary part of the input impedance of the single HSMS-282 diode is lower than that of the two series HSMS-282 diode. The real part of the input impedance of the series diodes varies more steeply with increasing input power within the range of interest. These characteristics can be used to design rectifiers with a power division strategy. By designing and optimizing the characteristic impedances and the lengths of the three transmission lines (from TL_1 to TL_3) carefully, the input microwave signal can be always rectified by the appropriate subrectifier. In this way, a high RF-DC conversion efficiency is maintained over an extended input power range.

1) Short-Circuit Stubs TL_1 and TL_3: A rectifier with $\lambda_g/8$ short-ended transmission line has been researched in our previous work [13], whose input impedance is inductive

$$Z_{\mathrm{IN1}} = jZ_1 \tan\left(\frac{\pi}{4}\frac{\omega}{\omega_0}\right) = \begin{cases} 0, & \omega = 0 \\ jZ_1, & \omega = \omega_0 \\ \infty, & \omega = 2\omega_0 \end{cases} \tag{7}$$

where Z_1 is the characteristic impedance of $\lambda_g/8$ short-ended transmission line. Then, it can be used to take place of L_1 and L_2 in Fig. 1 to reduce the imaginary part of the input impedances of both the single diode and the two series diodes at low and high powers, respectively.

2) Impedance Transformer TL_2: As shown in Fig. 5(a), the real part of the input impedance of the two series diodes is much higher than Z_0 when the input power is high. This impedance is equal to Re($Z_{IN}^{B'}$) because the series short-circuit stub TL_3 does not change the real part of the input impedance of the diodes. We can use the impedance transformation technique to transform Re(Z_{IN}^{B}) into Z_0 with a $\lambda_g/4$ transmission line, whose input impedance is given by [14]

$$Z_{\mathrm{IN2}} = \frac{Z_2^2}{Z_L} \tag{8}$$

where Z_2 and Z_{L} are the characteristic impedance and load of $\lambda_g/4$ short-ended transmission line, respectively. Additionally, Re(Z_{IN}^{B}) should be higher than Z_0 under low power conditions to reduce the power flowing to subrectifier B via careful selection of Z_{TL2}.

B. Simulation

Simulations were conducted for rectifier I to demonstrate the power division strategy. As shown in Fig. 6(a), the proposed rectifier realizes the power division strategy over a wide input power range. At low input power, subrectifier A receives more power than subrectifier B and vice versa.

The simulation results show that rectifier I realizes the proposed design concept, with subrectifier A and B working at various input power levels. The simulated conversion efficiency of the proposed rectifier I is compared with that of each individual subrectifier. The results are shown in Fig. 6(b). The overall rectifying efficiency is the higher one of either subrectifier A or B. The strategy shows subrectifier A and B are combined to broaden the operational power range greatly.

C. Implementation and Measurement

The proposed rectifier I is implemented and tested for experimental validation. The substrate is F4B with a thickness of 1 mm and a relative permittivity of 2.65. The layout and the detailed dimensions are presented in Fig. 7.

The simulation and measurement results are shown in Fig. 8(a). The measurement results agree well with the simulated results. Rectifier I maintains more than 50% efficiency when the power varies from 6.5 to 29.8 dBm. The rectifier features a 23.3 dB dynamic range with efficiency of more than 50%.

IV. Design and Measurement of Rectifier II

A. Design Methodology

Rectifier I has realized an extended input power range. The dynamic range of a rectifier using this power division strategy

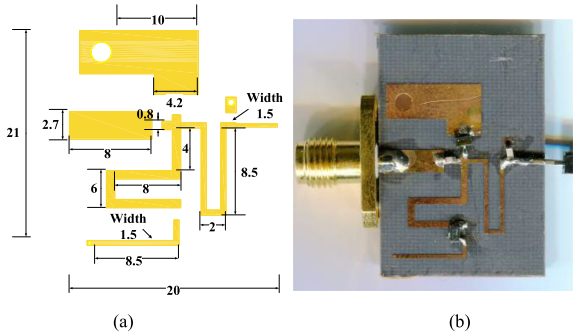

Fig. 7. Proposed rectifier I. (a) Layout. (b) Fabricated rectifier.

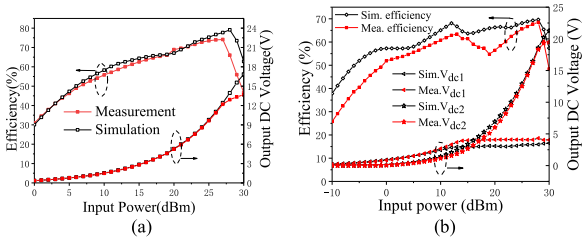

Fig. 8. Simulation and measurement of output dc voltage and RF-DC rectifying efficiency of the proposed rectifier (a) I and (b) II with input powers.

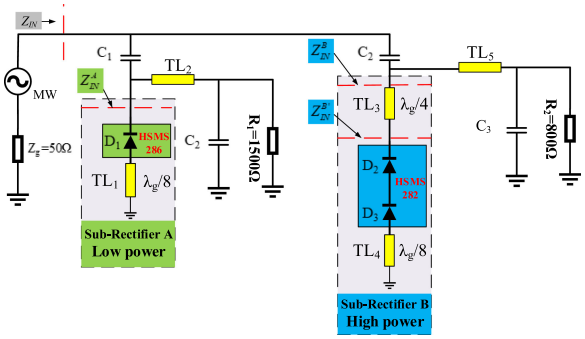

Fig. 9. Schematic of the proposed Rectifier II.

can be broadened further by selecting a different combination of diodes. Therefore, one single HSMS 286 diode and two series HSMS 282 diodes are applied at low-input power levels and high-input power levels, respectively. To avoid reverse breakdown of the HSMS 286 diode during high power rectification, two capacitors are used as dc blocking to isolate their bias voltages, as shown in Fig. 9. The proposed Rectifier I also contains three segments of transmission lines.

B. Implementation and Measurement

The proposed rectifier I with its extended input power range was implemented and measured for experimental validation. The same substrate was used. The layout and the detailed dimensions of the rectifier are presented in Fig. 10.

The simulated and measured results for the proposed rectifier I are plotted in Fig. 8(b). The figure shows that the measured conversion efficiency exceeds 50% over the input power range

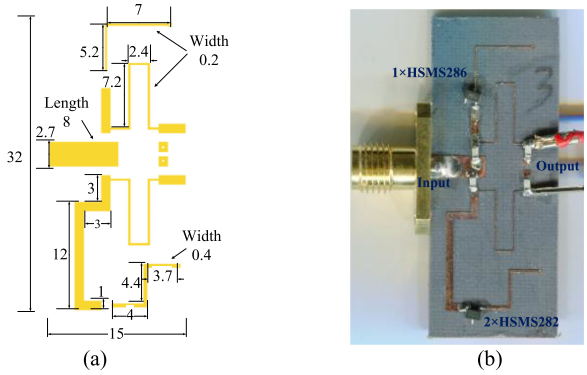

Fig. 10. Proposed Rectifier II. (a) Layout. (b) Fabricated rectifier.

TABLE I
Comparison With Prior Rectifiers

Ref.	Freq. (GHz)	Power range for efficiency>50%	Maximum efficiency	Dimensions	Year
[3]	2.45	10.5dBm–31.8dBm (21.3 dB)	80% @28dBm	82mm×66mm	2017
[4]	2.45	2.9dBm–20.2dBm (17.3 dB)	80.8% @17.2 dBm	126mm×68mm	2017
[10]	2.34	>13 dB	74.9% @16 dBm	95mm×62mm	2017
[11]	2.4	2.5dBm–25.5dBm (23 dB)	81.2% @20.5 dBm	30mm×19mm	2018
[9]	2.45	0.5dBm–18.5dBm (18 dB)	73.6% @14.1 dBm	43mm×35mm	2019
This work	**2.45**	**6.5dBm–29.8dBm (23.3 dB)**	**74.5% @27 dBm**	**20mm×21mm**	**2020**
This work	**2.45**	**−1dBm–30dBm (31 dB)**	**68.5% @28 dBm**	**15mm×32mm**	**2020**

from −1 to 30 dBm, which gives an extremely dynamic range of 31 dB. The maximum efficiency is 68.5% at an input power of 28 dBm.

Table I shows a comparison between the proposed rectifiers and several prior work. The proposed Rectifier I reaches the widest dynamic range for RF-dc conversion efficiency of more than 50%.

V. Conclusion

Two high-efficiency RF rectifiers with an extended input power range have been proposed that use the nonlinear impedance characteristics of diodes. The proposed power division strategy may be applied to other circuit designs when power division of different branches is required.

References

[1] S. Y. R. Hui, W. Zhong, and C. K. Lee, "A critical review of recent progress in mid-range wireless power transfer," *IEEE Trans. Power Electron.*, vol. 29, no. 9, pp. 4500–4511, Sep. 2014.

[2] B. L. Cannon, J. F. Hoburg, D. Stancil, and S. C. Goldstein, "Magnetic resonant coupling as a potential means for wireless power transfer to multiple small receivers," *IEEE Trans. Power Electron.*, vol. 24, no. 7, pp. 1819–1825, Jul. 2009.

[3] Z.-X. Du and X. Y. Zhang, "High-efficiency microwave rectifier with less sensitivity to input power variation," *IEEE Microw. Wireless Compon. Lett.*, vol. 27, no. 11, pp. 1001–1003, Nov. 2017.

[4] X. Y. Zhang, Z.-X. Du, and Q. Xue, "High-efficiency broadband rectifier with wide ranges of input power and output load based on branch-line coupler," *IEEE Trans. Circuits Syst. I, Reg. Papers*, vol. 64, no. 3, pp. 731–739, Mar. 2017.

[5] P. Lu, X. Yang, J. Li, and B. Wang, "A compact frequency reconfigurable rectenna for 5.2- and 5.8-GHz wireless power transmission," *IEEE Trans. Power Electron.*, vol. 30, no. 11, pp. 6006–6010, Nov. 2015.

[6] P. Lu, C. Song, and K. M. Huang, "A compact rectenna design with wide input power range for wireless power transfer," *IEEE Trans. Power Electron.*, vol. 35, no. 7, pp. 6705–6710, Jul. 2020.

[7] H. Matsumoto, N. Kaya, M. Fujita, Y. Fujino, T. Fujiwara, and T. Sato, "MILAX airplane experiment and model airplane," (in Japanese), in *Proc. 11th ISAS Space Energy Symp.*, 1993, pp. 47–52.

[8] K. Hamano *et al.*, "Wide dynamic range rectifier circuit with sequential power delivery technique," in *Proc. 12th Eur. Microw. Integr. Circuits Conf.*, Nuremberg, Germany, 2017, pp. 415–418.

[9] Y. Y. Xiao, J.-H. Ou, Z. X. Du, X. Y. Zhang, W. Che, and Q. Xue, "Compact microwave rectifier with wide input power dynamic range based on integrated impedance compression network," *IEEE Access,* vol. 65, pp. 151878–115188, Oct. 2019.

[10] M.-D. Wei, Y.-T. Chang, D. Wang, C.-H. Tseng, and R. Negra, "Balanced RF rectifier for energy recovery with minimized input impedance variation," *IEEE Trans. Microw. Theory Techn.*, vol. 65, no. 5, pp. 1598–1604, May 2017.

[11] P. Wu *et al.*, "High-efficient rectifier with extended input power range based on self-tuning impedance matching," *IEEE Microw. Wireless Compon. Lett.*, vol. 28, no. 12, pp. 1116–1118, Dec. 2018.

[12] J. O. McSpadden, L. Fan, and K. Chang, "Design and experiments of a high-conversion-efficiency 5.8-GHz rectenna," *IEEE Trans. Microw. Theory Techn.*, vol. 46, no. 12, pp. 2053–2060, Dec. 1998.

[13] C. Liu, F. Tan, H. Zhang, and Q. He, "A novel single-diode microwave rectifier with a series band-stop structure," *IEEE Trans. Microw. Theory Techn*, vol. 65, no. 2, pp. 600–606, Feb. 2017.

[14] D. M. Pozar, *Microwave Engineering*, 3rd ed. New York, NY, USA: Wiley, 2004.